Hypothermia Prevents Gliosis and Angiogenesis Development in an Experimental Model of Ischemic Proliferative Retinopathy

Manuel Rey-Funes,[1] Verónica Berta Dorfman,[2] Mariano Esteban Ibarra,[1] Elena Peña,[1] Daniela Soledad Contartese,[1] Jorge Goldstein,[3] Juan Manuel Acosta,[4] Ignacio M. Larráyoz,[5] Ricardo Martínez-Murillo,[6,7] Alfredo Martínez,[5,7] and César Fabián Loidl[1,4]

[1]Laboratorio de Neuropatología Experimental, Instituto de Biología Celular y Neurociencia "Prof. Eduardo De Robertis," Facultad de Medicina, Universidad de Buenos Aires, CONICET, Ciudad Autónoma de Buenos Aires, Argentina
[2]Centro de Estudios Biomédicos, Biotecnológicos, Ambientales y Diagnóstico (CEBBAD), Universidad Maimónides, Ciudad Autónoma de Buenos Aires, Argentina
[3]Departamento de Fisiología, Facultad de Medicina, Universidad de Buenos Aires, CONICET, Ciudad Autónoma de Buenos Aires, Argentina
[4]Laboratorio de Neurociencia, Facultad de Ciencias Médicas, Universidad Católica de Cuyo, San Juan, Argentina
[5]Angiogenesis Study Group, Center for Biomedical Research of La Rioja (CIBIR), Logroño, Spain
[6]Neurovascular Research Group, Department of Molecular, Cellular and Developmental Neurobiology, Instituto Cajal, (CSIC), Madrid, Spain
[7]Unidad Asociada CIBIR-CSIC, Logroño, Spain

Correspondence: César Fabián Loidl, "Laboratorio de Neuropatología Experimental," Instituto de Biología Celular y Neurociencia "Prof. Eduardo De Robertis," Facultad de Medicina, Universidad de Buenos Aires - CONICET, Paraguay 2155 3°Piso, Ciudad Autónoma de Buenos Aires, Argentina; cfloidl@yahoo.com.ar.

Submitted: October 24, 2012
Accepted: January 14, 2013

Citation: Rey-Funes M, Dorfman VB, Ibarra ME, et al. Hypothermia prevents gliosis and angiogenesis development in an experimental model of ischemic proliferative retinopathy. *Invest Ophthalmol Vis Sci.* 2013;54:2836–2846. DOI:10.1167/iovs.12-11198

Purpose. To develop a time course study of vascularization and glial response to perinatal asphyxia in hypoxic-ischemic animals, and to evaluate hypothermia as possible protective treatment.

Methods. We used retinas of 7-, 15-, 21-, and 30-day-old male Sprague-Dawley rats that were exposed to perinatal asphyxia at either 37°C (PA) or 15°C (HYP). Born to term animals were used as controls (CTL). We evaluated the thickness of the most inner layers of the retina (IR), including internal limiting membrane, the retinal nerve fiber layer, and the ganglion cell layer; and studied glial development, neovascularization, adrenomedullin (AM), and VEGF by immunohistochemistry, immunofluorescence, and Western blot.

Results. A significant increment in IR thickness was observed in the PA group from postnatal day (PND) 15 on. This alteration was concordant with an increased number of new vessels and increased GFAP expression. The immunolocalization of GFAP in the internal limiting membrane and perivascular glia of the IR and in the inner processes of Müller cells was coexpressed with AM, which was also significantly increased from PND7 in PA animals. In addition, VEGF expression was immunolocalized in cells of the ganglion cell layer of the IR and this expression significantly increased in the PA group from PND15 on. The retinas of the HYP group did not show differences when compared with CTL at any age.

Conclusions. This work demonstrates that aberrant angiogenesis and exacerbated gliosis seem to be responsible for the increased thickness of the inner retina as a consequence of perinatal asphyxia, and that hypothermia is able to prevent these alterations.

Keywords: retina, ischemic proliferative retinopathy, retinopathy of prematurity, angiogenesis, gliosis, hypothermia, perinatal asphyxia

Perinatal asphyxia (PA) is the world's most severe problem in perinatology services.[1,2] It generates a global transient hypoxia-ischemia status that damages the brain, spinal cord, and retina.[3–8] The degree and the length of PA are decisive for the development of injury sequelae, such as attention-deficit hyperactivity disorder,[9] epilepsy, mental retardation, spasticity, and visual or hearing alterations.[10] A third of asphyctic neonates develop serious long-term neurological injuries, including several degrees of ischemic proliferative retinopathy (IPR).[11]

We have described that adult animals (60 days old) that have been exposed to PA develop retinal morphological changes that are compatible with some alterations observed in diseases, such as retinopathy in diabetes mellitus, retinal vein occlusion, and retinopathy of prematurity (ROP), an avoidable cause of visual impairment and blindness in children.[10–13] The changes observed in asphyctic animals include ganglion cell degeneration, neovascularization of the most inner layers of the retina (IR) (including the internal limiting membrane, the retinal nerve fiber layer, and the ganglion cell layer), and Müller cell hypertrophy in the inner half layers of the retina (including the inner nuclear layer, the inner plexiform layer [IPL], the internal limiting membrane, the retinal nerve fiber layer, and the ganglion cell layer), with

Investigative Ophthalmology & Visual Science

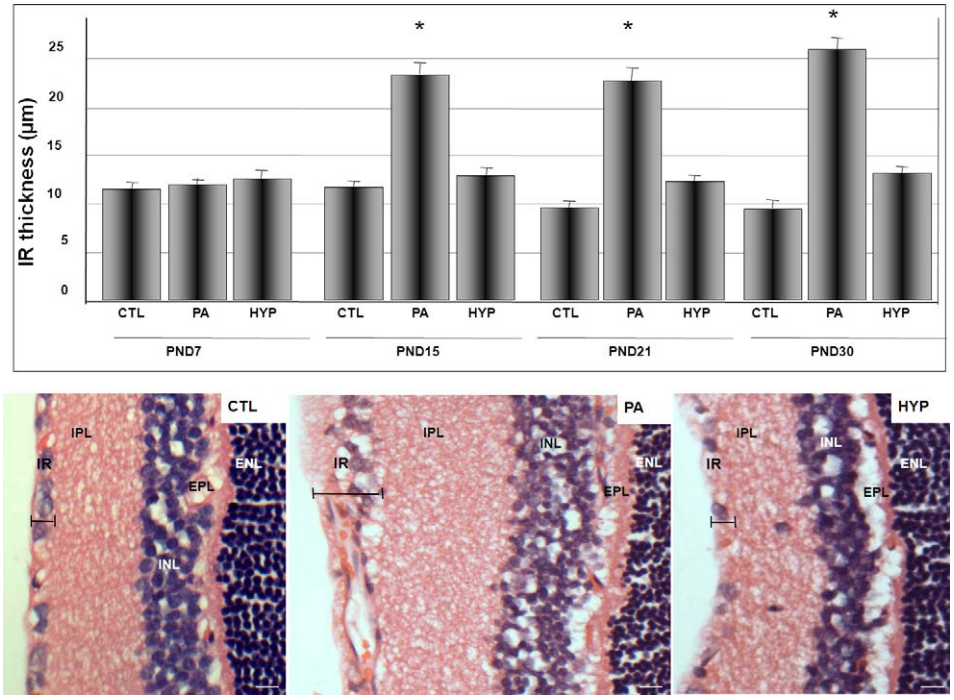

Figure 1. Perinatal asphyxia increases the thickness of the IR throughout time. Thickness was measured in hematoxylin-eosin–stained slides. Significant increase of the thickness of the IR was observed in the PA group when the animals were 15 days of age and older. The thickness of the IR was not modified in the HYP group with respect to the CTL group. *Upper panel*: time course graph of IR thickness for the four evaluated groups. Each *bar* represents the mean ± SD of six sections per animal in five animals per group. $^*P < 0.05$ versus CTL at the same age. *Lower panel*: representative hematoxylin-eosin images of 30-day-old CTL, PA, and HYP retinas. Caliber shows IR thickness. IR includes the internal limiting membrane, the retinal nerve fiber layer, and the ganglion cell layer. INL, inner nuclear layer; EPL, external plexiform layer; ENL, external nuclear layer. *Scale bars*: 20 µm.

significant increased expression of glial fibrillary acidic protein (GFAP) in activated Müller cells.[7]

Animal studies have shown that a reduction in core temperature protects the nervous system against ischemic damage by a reduction of the metabolism, decreasing reactive oxygen species, and inhibiting the toxic release of nitric oxide (NO).[3,5,8,14,15] Hypothermia during PA prevents central nervous system (CNS) damage when compared with animals kept under normothermic conditions.[3,5,8] According to our previous studies, when asphyxia occurs at low temperature (15°C) there are no deaths among neonates, whereas the same procedure performed at 37°C results in 60% pup mortality.[5,16] The use of hypothermia has been proposed as a treatment to reduce secondary neuronal injury after severe perinatal hypoxia-ischemia in humans.[15,17–19]

Adrenomedullin (AM) is a peptide hormone initially isolated from extracts of human pheochromocytoma.[20] It is involved in the induction of vasodilatation, regulation of cell proliferation, and angiogenesis.[21] The expression and secretion of this peptide are induced by inflammatory cytokines and hypoxia through activation of hypoxia inducible factor 1 (HIF-1). Under low oxygen pressure conditions (<2%), transactivation of the AM promoter with increased translation of AM peptide was observed.[22] In the CNS, AM is secreted by neurons and glia.[23] AM is also expressed in RPE, in the aqueous humor, and in the vitreous of human patients with proliferative vitreoretinopathy,[24] diabetic retinopathy,[25] and uveitis or vitreoretinal disorders.[26] A full description of the cellular populations that express AM in the rat retina is not available, and its pathophysiological role in hypoxia-ischemia is not yet well understood.

Development of retina vascularization, under physiological or pathophysiological conditions, is a complex process that involves different factors, such as VEGF.[27] Increased levels of VEGF were identified in models of retinal ischemia.[28] The key factor regulating angiogenesis in response to hypoxia is likely to be HIF-1, whose activation stimulates the production of VEGF.[27,29]

Considering that PA induces the thickening of the IR and the presence of newly formed vessels in adult hypoxic/ischemic animals,[7] the aim of the present work was to evaluate the impact of hypoxia-ischemia in a time course study analyzing the changes induced by PA in the retinal structure. We specially focused on the development of retinal damage elicited by vascularization and gliosis, the study of the expression and distribution of pro-angiogenic factors, such as AM and VEGF, and the application of hypothermia as a neuroprotective treatment.

Materials and Methods

Hypoxic-Ischemic Injury

Severe PA was induced using a noninvasive model of hypoxia-ischemia, as described.[6] Sprague-Dawley albino rats with genetic quality and sanitary certification from the animal facility of our institution were cared for in accordance with the guidelines published in the ARVO Statement for the Use of Animals in Ophthalmic and Vision Research, and in the National Institutes of Health (NIH) *Guide for the Care and Use of Laboratory Animals* (NIH Publication No. 85-23, revised 1985, available from: Office of Science and Health Reports, National Center for Research Resources, Bethesda, MD), and the principles presented in the "Guidelines for the Use of Animals in Neuroscience Research" by the Society for Neuroscience (available from the Society for Neuroscience,

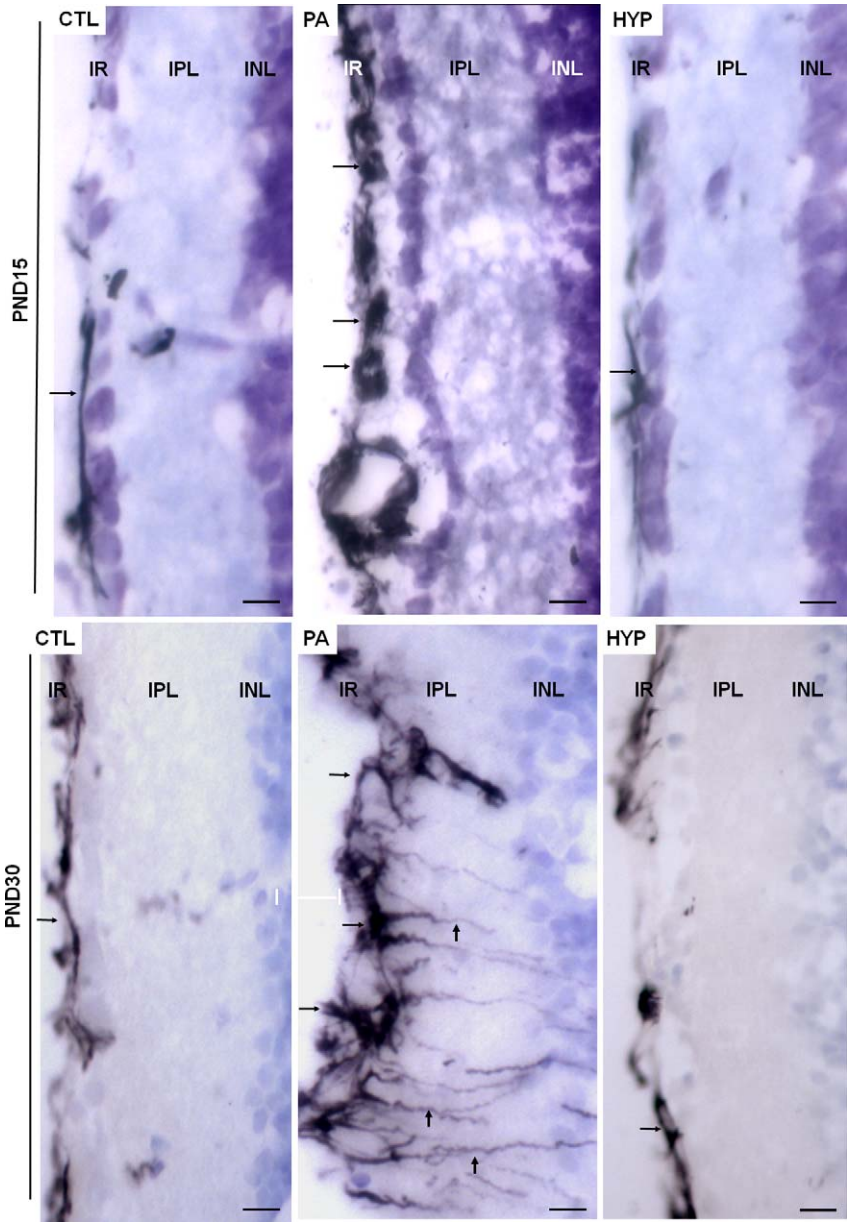

Figure 2. Increase of GFAP expression induced by PA and reversion by HYP. Representative images of GFAP immunolocalization in the IR of CTL, PA, and HYP animals that were 15 (*top*) and 30 days of age (*bottom*). Increased GFAP expression was observed in Müller cells of PA of both ages and was significantly increased with respect to CTL. HYP retinas did not show differences when compared with the CTL retinas. PA-15PND animals showed GFAP immunolocalization at perivascular glial cells (*horizontal arrows*) localized in the IR, whereas PA-30PND rats showed GFAP immunoreactivity also at glial processes of the retinal IPL and INL (*vertical arrows*). IR includes the internal limiting membrane, the retinal nerve fiber layer, and the ganglion cell layer. *Scale bars*: 10 μm.

Washington, DC; published in the Membership Directory of the Society, pp. xxvii–xxviii, 1992). The animal model described below was approved by the Ethical Committee of CICUAL (Comité Institucional para el Uso y Cuidado de Animales de Laboratorio) (Resolution No. 2079/07), Facultad de Medicina, Universidad de Buenos Aires, Argentina. Appropriate proceedings were performed to minimize the number of animals used and their suffering, pain, and discomfort. Animals were kept under standard laboratory conditions at 24°C, with light/dark cycles of 12/12 hours, and food and water were given ad libitum. Thirty-two timed-pregnant Sprague-Dawley rats were killed by decapitation and immediately hysterectomized after their first pup was delivered vaginally. These normally delivered, nonmanipulated pups were used as controls (CTLs; $n = 5$ per group). Full-term fetuses, still inside the uterus, were subjected to asphyxia performed by transient immersion of both uterine horns in a water bath for 20 minutes at either 37°C (PA; $n = 5$ per group) or at 15°C (HYP; $n = 5$ per group). For the hypothermia group, the temperature of 15°C was chosen because it allows the highest pup survival rate.[16,30] After asphyxia, the uterine horns were opened, pups were removed, dried of delivery fluids, stimulated to breathe, and their umbilical cords were ligated. The pups were then placed for recovery under a heating lamp and given to a surrogate mother. Time of asphyxia was measured as the time elapsed from the hysterectomy up to the recovery from the water bath. The overall mortality rate was similar to that previously reported,[6]

Investigative Ophthalmology & Visual Science

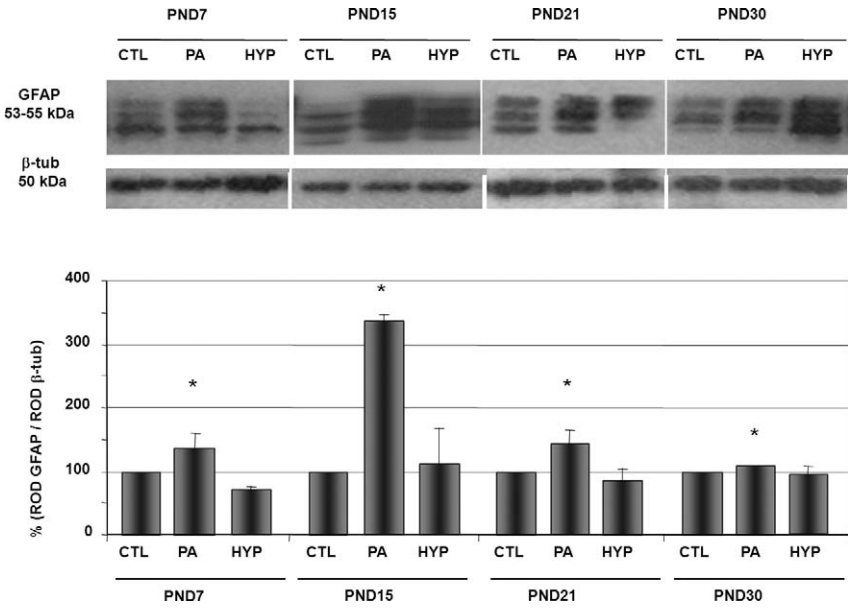

Figure 3. Increase in astroglia markers was induced by PA and reversed by HYP. Western blot analysis of GFAP expression. PA group showed increased GFAP expression levels with respect to CTL in all age groups studied. In contrast, GFAP expression in the HYP group did not show significant differences when compared with CTL of the same age. *Upper panel*: representative images of Western blots assays. β-tubulin was used as a loading control. *Lower panel*: quantification of GFAP levels. $^*P < 0.05$ versus CTL at the same age.

60% for the PA group and 0% for the HYP group. To avoid the influence of hormonal variations due to the female estrous cycle, only male rats were included in this study.

Tissue Processing and Measurement of Retinal Thickness

CTL, PA, and HYP rats of 7, 15, 21, and 30 days of age (postnatal day [PND]7, PND15, PND21, and PND30, respectively) were intraperitoneally anesthetized with chloral hydrate 28% weight/volume (0.1 mL/100 g body weight) and intracardially perfused with physiological solution followed by 4% paraformaldehyde in 0.1 M, pH 7.4, phosphate buffer at 4°C. After enucleating, anterior segments of the eyes, including the lens, were discarded, and the posterior segments of the eyes containing the retinas were post-fixed overnight in the same fixative at 4°C. Following cryoprotection with growing series of sucrose (10%, 20%, and 30%) in PBS at 4°C overnight, tissues were included in Tissue-Tek OCT (Sakura, Alphen aan den Rijn, The Netherlands), frozen in powdered dry ice, and stored at –80°C. Sections (15-μm thick) were obtained using a Leitz "Lauda" cryostat (Leica Biosystems, Germany) and mounted onto gelatin-coated slides (2.5% gelatin, 1% Elmer's glue [Elmer's Products, Inc., Columbus, OH]), air dried at room temperature, and stored at –80°C until their use. For retinal thickness measurements, hematoxylin-eosin staining was performed and the thickness of the IR, which includes the internal limiting membrane, the retinal nerve fiber layer, and the ganglion cell layer, was measured.

Immunohistochemistry

For immunohistochemical assays, endogenous peroxidase activity was blocked with 1% hydrogen peroxide in phosphate buffer for 30 minutes. Then, sections were incubated with blocking solution containing 10% normal goat serum in PBS, pH 7.4, for 1 hour. Slides were incubated with a rabbit polyclonal anti-AM antibody (at dilution 1:1000, according to Garayoa et al.[22]), a mouse monoclonal anti-GFAP antibody (dilution 1:500; Sigma-Aldrich, St. Louis, MO), or a rabbit polyclonal anti-VEGF antibody (dilution 1:1000; Santa Cruz Biotechnology, Santa Cruz, CA). Antibodies were incubated overnight at 4°C and their specificity corroborated in adjacent sections by omission of primary antibodies. Immunoreactivity was visualized with biotinylated goat antirabbit or antimouse IgG (1:100; Sigma-Aldrich), developed with ABC kit (Vector Laboratories, Burlingame, CA) and 0.03% 3,3′diaminobenzidine (Sigma-Aldrich), 3% nickel ammonium sulfate (Merck, Darmstadt, Germany), and 0.01% hydrogen peroxide diluted in 0.1 M buffer acetate, yielding a black product. Sections were dehydrated, cleared, and mounted. For colocalization studies, the anti-AM rabbit polyclonal IgG at dilution 1:1000 and the anti-GFAP monoclonal mouse IgG at dilution 1:500 were employed. Following overnight incubation with both primary antibodies, colocalization studies were performed by immunofluorescence technique using Alexa fluor 555 coupled antirabbit IgG (dilution 1:300; Life Technologies, Carlsbad, CA) and FITC-coupled antimouse IgG (at dilution 1:300; Vector Laboratories). Counterstaining of nuclei was made with 4′-6-diamidino-2-phenylindole (DAPI) (1:1000; Sigma-Aldrich) to identify cellular localization.

Tomato Lectin Histochemistry

To study vessel distribution, some retina sections were stained with biotinylated *Lycopersicum esculentum* (tomato) lectin (Sigma-Aldrich) at a 1:150 dilution and revealed with an ABC kit followed by diaminobenzidine-Nickel. After the histochemical process, some slides were counterstained with cresyl violet.

SDS-PAGE and Western Blotting

The retinas of CTL, PA, and HYP animals of 7, 15, 21, and 30 days of age (PND7, PND15, PND21, PND30, respectively) were dissected, frozen, and stored at –80°C until used. Tissues were homogenized (1:3, wt/vol) in HEPES buffer (20 mM *N*-[2-hydroxethyl]piperazine-*N*′-[2-ethanesulfonic acid], pH 7.2, containing 0.2 M sucrose, 1 mM EDTA, 5 mM dithiothreitol,

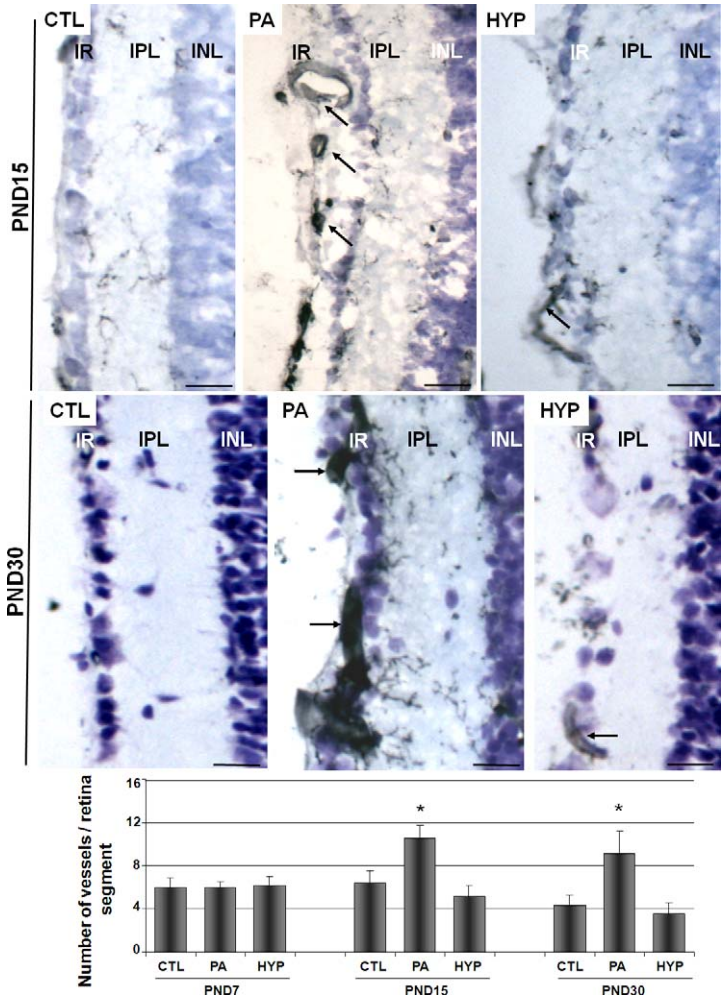

Figure 4. Increased vascularization induced by PA and reversion by HYP. Images are representative of tomato lectin histochemistry in PND15 and PND30 retinas. Vessels with both small and large diameter (*arrows*) were observed in the IR of the PA group at both PND15 and PND30. IR is the layer conformed by the internal limiting membrane, the retinal nerve fiber layer, and the ganglion cell layer. *Scale bar*: 40 μm. The graphic shows the significantly increased number of vessels observed in PND15 PA and PND30 PA groups when compared with CTL groups (*$P < 0.05$). PND7 did not show significant changes in the number of vessels among groups. HYP treatment reverted blood vessel density to normal values.

10 μg/mL soybean trypsin inhibitor, 10 μg/mL leupeptin, 2 μg/mL pepstatin, and 0.1 mM phenylmethylsulfonyl fluoride). All procedures were carried out at 4°C. Homogenates were centrifuged for 30 minutes at 15,000*g* and the supernatants collected. In order to use similar amounts of proteins from each sample (25 μg), protein concentration was determined by the Bradford method, with bovine serum albumin as standard, using a NanoDrop spectrophotometer (ND100; Thermo, Wilmington, DE). Then, supernatant samples were mixed 1:1 with sample buffer (10 mL Tris-HCl 0.5 M, pH 6.8, 16 mL SDS 10% [wt/vol], 8 mL glycerol, 2 mL 2-mercaptoethanol, and 0.2 mL bromophenol blue 0.1% [wt/vol]) and heated for 3 minutes at 95°C. Samples were run on SDS–polyacrylamide gels (10% running gel with 3.5% stacking gel), with 0.25 M Tris–glycine, pH 8.3, as the electrolyte buffer, in a Bio-Rad Mini-Protein II (Bio-Rad, Madrid, Spain). Kaleidoscope prestained standards (Bio-Rad) were used as molecular weight markers. For Western blot analysis, proteins were transferred at 1.5 mA/cm^2 for 1 hour onto 0.2-μm polyvinylidene difluoride (PVDF) membranes (Immobilon-P; Millipore, Bedford, MA) by semi-dry transfer methods (Bio-Rad). For protein identification, membranes were incubated overnight at 4°C with the rabbit polyclonal anti-AM IgG at dilution 1:1000 or with the mouse monoclonal anti-GFAP antibody at dilution 1:1000. To standardize the results, monoclonal IgG anti-β-tubulin (Sigma-Aldrich) was used at dilution 1:10,000 in the same membranes. To visualize immunoreactivity, membranes were incubated with antirabbit or antimouse peroxidase-labeled IgGs, developed with a chemoluminiscence kit (GE Biosciences, Miami, FL), and exposed to x-ray blue films (CEA, Strängnäs, Sweden). Developed films were scanned with a computer-assisted densitometer (GS-800; Bio-Rad) and optical density quantified by NIH Scion Image software (developed by Wayne Rasband, 1995, NIH, Research Services Branch, NIMH, Bethesda, MD).

Image Analysis

Six retinal sections from five animals of each experimental group were analyzed. Care was taken on selecting anatomically matched areas of retina among animals before assays. Relative optical density (ROD), immunoreactive cellular area, and number of immunoreactive cells (or tomato lectin reactive vessels) were analyzed using an Olympus BH2 microscope (Olympus Optical Corporation, Tokyo, Japan) attached to a video camera (CCD; Sony-XC77, San Diego, CA) and coupled to a computer equipped with a video card (Data Translation, Marlboro, MA). The central area of the sagittal plane was

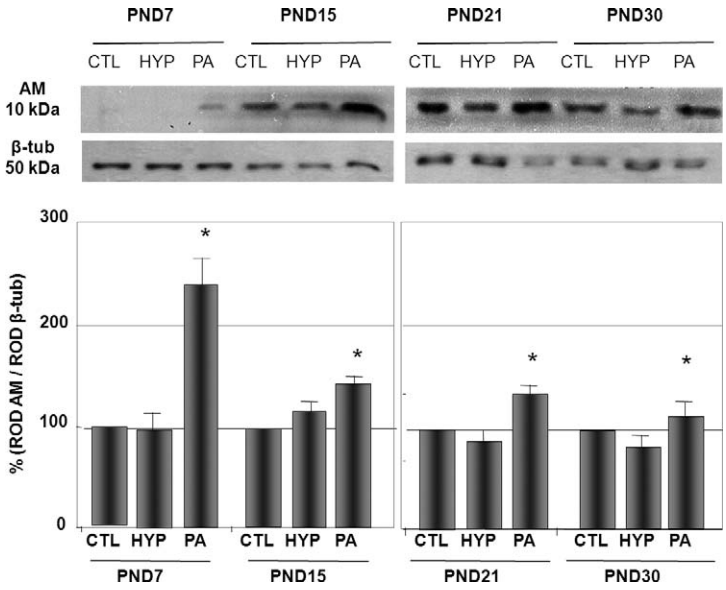

Figure 5. PA induces higher AM expression in Müller cells, and reversion by HYP. Representative images of AM immunolocalization (*red color*) in the IR of CTL, PA, and HYP animals of 15 (*top*) and 30 days of age (*middle*). Increased AM expression was observed at PA of both ages with respect to CTL. HYP did not show significant differences when compared with CTL. AM was localized in Müller cells of the IR, and along glial processes at IPL and INL. Nuclei were localized by DAPI staining (*blue*). IR is the layer conformed by the internal limiting membrane, the retinal nerve fiber layer, and the ganglion cell layer. Nuclei were counterstained with DAPI (*blue*). *Scale bars*: 15 μm. The graphic shows significantly increased ROD observed in PND15 PA and PND30 PA groups when compared with CTL groups (*$P < 0.05$). No changes were observed in HYP.

chosen for each retina. Thickness of the IR, including the internal limiting membrane, the retinal nerve fiber layer, and the ganglion cell layer, was measured. Mean thickness of a 160-μm length of retina segment was measured, and 10 fields per each retina were studied. Results show the thickness mean value of 10 fields. Scion Image software (NIH) was used to measure IR area thickness and to evaluate reactivity and immunoreactivity. Only those cells that had a gray level darker than a defined "threshold" criteria (defined as the optic density 3-fold higher than the mean background density) were considered specific immunoreactively stained cells. The mean background density was measured in a region devoid of immunoreactivity, immediately adjacent to the analyzed region. ROD was calculated using a gray scale of 255 gray levels. To avoid external variations, all images were taken the same day and under the same light. The number of cells was measured in retina segments of exactly 160 μm in length. Four segments were measured in each retinal section. Because immunohistochemistry and Western blotting are semiquantitative techniques, ROD values were expressed as percentage of change with respect to the CTL group, considering CTL's ROD as 100%. Colocalization was studied by immunofluorescence using a Nikon C1 Plus laser microscope (Nikon Inverted Research Microscope Eclipse Ti; Nikon Corp., Tokyo, Japan) and images analyzed with the EZ-C1 software (EZ-C1 Software v3.9; Nikon Corp.). Adobe Photoshop software (Adobe Photoshop CS5; Adobe Systems, Inc., Ottawa, ON, Canada) was used for digital manipulation of only brightness and contrast when preparing the shown images.

Statistical Analysis

Values are expressed as mean ± SD. At least two similar separate experiments were evaluated in all cases. Twelve sections of each animal were analyzed. Results were evaluated using one-way ANOVA and comparisons between groups were made by Fisher, Scheffe, and Bonferroni-Dunn tests, using the GraphPad software (GraphPad Software, San Diego, CA). Differences were considered significant when P was less than 0.05.

Results

The Thickness of the Most Inner Layers of the Retina Increases Throughout Time by Perinatal Asphyxia

Structural changes were evidenced in the IR of the PA group when compared with the CTL group, considering IR as the layer conformed by the internal limiting membrane, the retinal nerve fiber layer, and the ganglion cell layer. A significant increase in the thickness of the IR was observed in PA animals with respect to CTL at 15 days of age, and this increment was maintained in up to 30-day-old animals (Fig. 1). HYP prevented retinal thickening and the values from these retinas were undistinguishable from the control group (Fig. 1).

Increases in Astroglia and New Vessel Development Are Responsible for Thickening of the IR

Astroglial state of the retina was evaluated by GFAP immunohistochemistry and Western blotting in the retinas of rats from 7 to 30 days of age (Figs. 2, 3). A significant increase in GFAP expression was observed in retinas of the PA group when compared with those of CTL animals at all evaluated ages, whereas no alterations were observed in HYP with respect to CTL (Fig. 3). The maximum difference in GFAP expression was observed at PA-PND15 both by immunohistochemistry (Fig. 2) and by Western analysis (Fig. 3), where a 237% ± 10% increment was seen for this time period (Fig. 3). GFAP immunoreactivity was located in the internal limiting membrane and in the perivascular glial cells of the IR in the PA-PND15 group (Fig. 2). In older animals (PND30), GFAP expression was also observed in the internal processes of

Investigative Ophthalmology & Visual Science

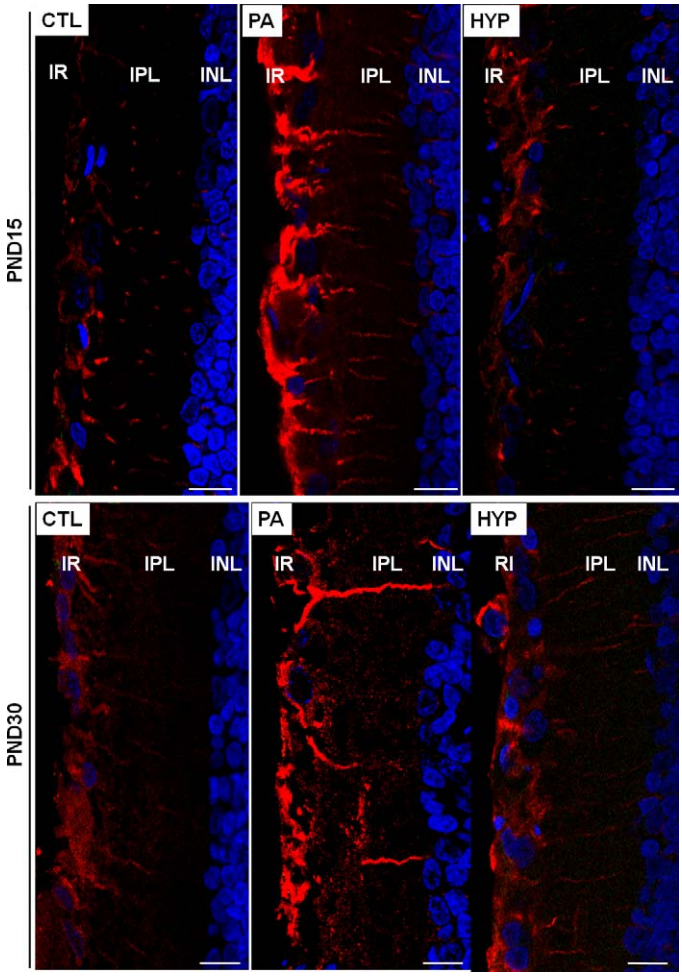

Figure 6. Increased AM expression was induced by PA and reverted by HYP. Western blot analysis of the expression of AM in the experimental groups. The PA group showed increased AM expression levels with respect to the CTL group in all age groups. The HYP group did not show significant differences in relation to the CTL group. *Top*: representative images of Western blot assays. β-tubulin was used as a loading control. *Bottom*: quantification of AM levels. $^{*}P < 0.05$ significant versus CTL at the same age.

Müller cells, crossing the IPL (Fig. 2). Alterations in neither localization nor protein expression levels were found in the HYP group when compared with the CTL animals at any of the evaluated ages (Figs. 2, 3).

The vascularization of the IR was studied by tomato lectin histochemistry. Increased vascularization was observed in PA with respect to CTL. A significant increment of 103% ± 11% ($P < 0.01$) in the number of vessels in the retina of PA-PND15 was observed compared with their normoxic counterparts (Fig. 4), and this increase was maintained at PND30. No differences were observed in the number of retinal vessels between CTL and HYP at any evaluated age (Fig. 4).

Effect of PA on the Expression of Retinal Angiogenic Factors

AM expression in the retina was evaluated by immunofluorescence and Western blotting. AM expression was detected in the processes of Müller cells of the IPL and in the IR from 15-day-old rats onwards (Fig. 5). After performing morphometric studies of AM expression, a significant increase on ROD was detected in the IR of PA-PND15 with respect to CTL-PND15 animals (90% ± 13%, $P < 0.05$). A similar pattern was observed in the PND30 group (112% ± 6%, $P < 0.05$) (Fig. 5). HYP animals showed no significant differences in comparison with CTL for any studied age. Western blot of AM expression showed that PND15 animals had a higher expression of this peptide than younger rats (Fig. 6). CTL-PND15 animals showed a significant 152% ± 13% increase ($P < 0.05$) when compared with the CTL-PND7 group. All PA groups showed significant AM expression increment in relation to CTL animals (PND7 = 143% ± 33%, PND15 = 42% ± 3%, PND21 = 51% ± 5%, and PND30 = 22% ± 11%, $P < 0.05$) (Fig. 6). Hypothermic treatment showed to be effective for the prevention of increased AM expression, resulting in no differences with respect to CTL.

Confocal immunofluorescence was used to perform colocalization studies between AM and GFAP. Colocalization of both immunoreactivities was found in the processes of Müller cells of the IPL and in the IR for rats that were 15 days old or older (Fig. 7). The PA group showed a concomitant increase in AM and GFAP immunofluorescent area, whereas similarities in the immunofluorescent colocalizing area were observed between CTL and HYP retinas (Fig. 7).

Expression and immunolocalization of VEGF were studied in the retinas of PND15 and PND30 rats. VEGF distribution was observed in the soma of cells in the ganglion cell layer of the IR. Morphometric studies revealed that the PA-PND15 group showed a significant 98% increase in the number of VEGF immunoreactive neurons, a significant 61% increment in the

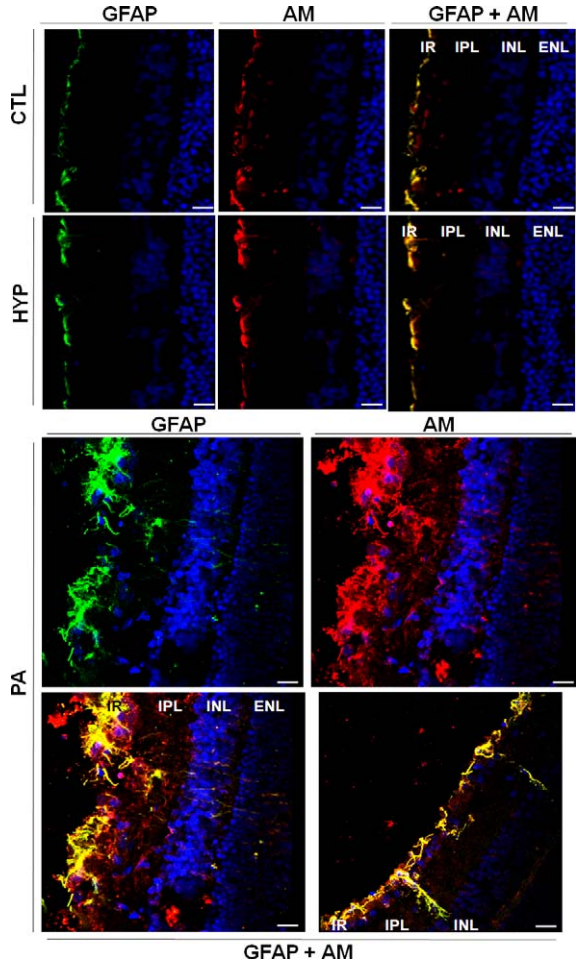

Figure 7. Colocalization of AM and GFAP in the IR. Representative images of AM (*red*) and GFAP (*green*) colocalization (*yellow*) in the most inner layers of the retina (IR) of PND30 animals. *Top*: low expression of both AM and GFAP in animals of the CTL and HYP groups. *Bottom*: colocalization and high expression of AM and GFAP in the IR of PA animals. IR includes the internal limiting membrane, the retinal nerve fiber layer, and the ganglion cell layer. Nuclei were counterstained with DAPI (*blue*). *Scale bars*: 50 μm.

VEGF immunoreactive cell area, and a significant 7% increased VEGF ROD with respect to CTL at PND15 (Fig. 8). PA-PND30 retinas showed similar VEGF alterations than PA-PND15 with respect to CTL in the three parameters examined (Fig. 8). Both evaluated ages showed no significantly different VEGF morphometric values between HYP and CTL retinas (Fig. 8).

Discussion

In the present study, we have shown that animals that had suffered PA develop a significant increase in the thickness of the IR, and that this occurs as a result of at least two factors: exacerbation of astroglial response and formation of new blood vessels. The finding that retinal changes occur at an early postnatal time is very relevant, opening the possibility for a therapeutic window.

The exposure to hyperoxia in neonatal intensive care preterm infants produces a high susceptibility to develop neurological and retinal injuries that include varying degrees of IPR.[7] Perinatal asphyxia in rats has proved to be a useful model for studying retinopathy,[7,8] as the induction of hypoxia-ischemia in the perinatal period produces morphological, biochemical, and molecular changes. The development of the rat CNS at birth is equivalent to the one found in human fetuses at 32 weeks of gestation.[12] Therefore, the model of asphyxia used in the present work offers the possibility of studying changes that may occur in the premature human CNS, including the retina.

In a previous work, we described, at structural and ultrastructural levels, alterations produced by PA in the IR of 60-day-old animals. These included formation of new vessels, and hypertrophy of Müller cells and perivascular astroglia.[7] We also observed increased enzymatic NO synthase (NOS) activity and age-dependent expression of NOS in hypoxic retinas.[8] Here we describe age-dependent alterations in the inner half layers of the retina produced by PA because of an early formation of vessels and an early expression of AM and GFAP in the hypoxic retinas.

The most important functions of AM are the induction of vasodilatation, regulation of cell proliferation, and angiogenesis.[21] Recently, AM localization in Müller cells of mouse retina and its signaling pathway has been described.[31] The localization of AM in the inner processes of Müller cells may be related to the promotion of angiogenesis in the IR. Under hypoxic conditions, AM may protect the retina through its vasodilatory activity; however, when animals are subjected to PA, a severe AM increase is detected. Significant alterations of AM expression were observed in 7-day-old retinas of asphyctic animals. Although this increase may activate angiogenesis development, new vessel construction shall demand more time being observed later, at 15 days of age. Our results suggest the possible action of AM in retina promoting vascularization development. To establish the exact developmental moment when AM stimulates angiogenesis, future efforts will be focused on the study of genomic responses of the hypoxic retina.

These results suggest that AM may be a pharmacological target to intervene in children in high risk of developing retinopathy. Several inhibitors of AM function have been described. These include a monoclonal antibody,[32] the peptide fragment AM 22-52,[33] and a series of small molecules.[34,35] All these potential drugs need to be tested first in animal models to confirm their efficacy in preventing retinopathy. The recent resolution of the three-dimensional structure of the AM peptide may help in the rational development of new drugs that target this system.[36]

AM, VEGF, and inducible NOS (iNOS) expression are all stimulated by HIF-1.[22,27,37] The IRs are particularly sensitive to changes in oxygen levels,[27,38] causing various degrees of retinopathy that in some cases can lead to blindness. NO is postulated as a key factor in the neurotoxicity of ROP,[8,27] and its elevated concentration produces cytotoxic effects on the retina.[7,38,39] Other studies also showed that angiogenesis stimulated by hypoxia is linked to increased transcription of HIF-1.[40] In normoxia, HIF-1 α is hydroxylated and its degradation ensues, but in hypoxia, HIF-1 α is not hydroxylated, allowing its translocation to the nucleus where it dimerizes with HIF-1 β and acts as a transcription factor for target genes, which include iNOS,[27] VEFG,[37] and AM.[22]

The development of vascularization in the retina is controlled by interactions between ganglion cells, astrocytes, and endothelial cells. Ganglion cells secrete platelet-derived growth factor (PDGF-A) to stimulate astrocyte proliferation, which in turn promotes secretion of VEGF.[41] VEGF signaling pathway plays a central role modulating the vascularization of the retina. In our model of PA, we observed that hypoxia induces a significant increase in VEGF expression in cells of the ganglion cell layer of the IR, and this increment would be involved in angiogenesis promotion. Similar results have been

Investigative Ophthalmology & Visual Science

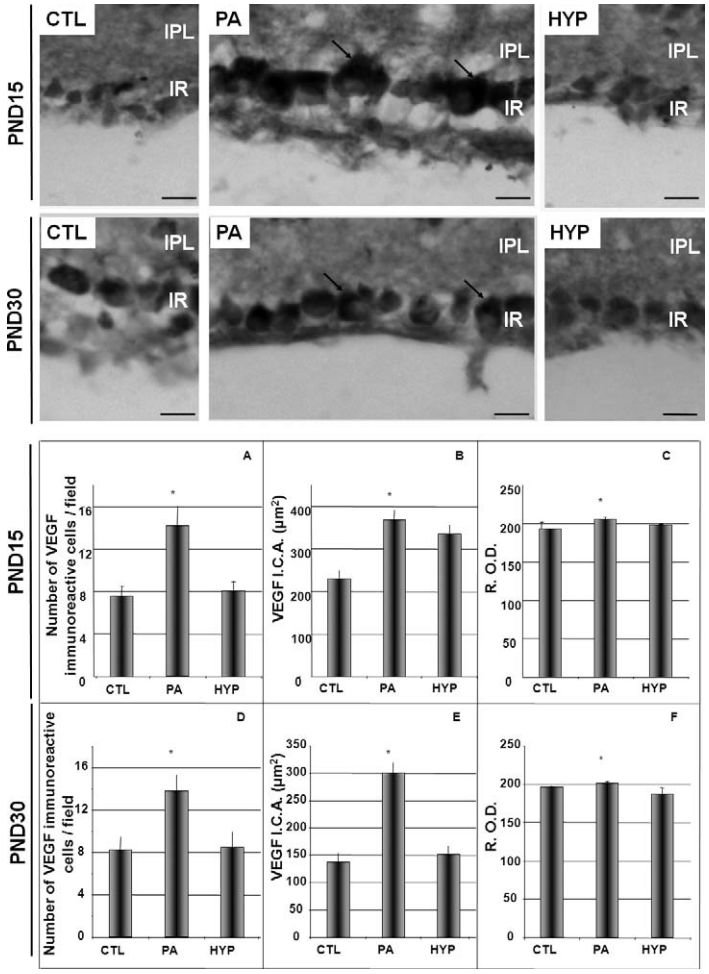

Figure 8. Increased expression of VEGF in the IR induced by PA and reversion by hypothermia. *Top*: representative images of VEGF immunolocalization in cells of the ganglion cell layer of the IR in CTL, PA, and HYP animals of 15 and 30 days of age. Increased VEGF expression (*arrows*) was observed in PA animals of both ages when compared with the CTLs. HYP did not show significant differences in VEGF expression as it relates to CTL. IR is the layer conformed by the internal limiting membrane, the retinal nerve fiber layer, and the ganglion cell layer. *Scale bars*: 10 µm. *Bottom*: morphometric values of the number of VEGF immunoreactive cells per field, VEGF ICA, and ROD. Significant increments were observed in all PA groups with respect to CTL at all evaluated parameters. The HYP group did not show significant differences with respect to CTL. $^{*}P < 0.05$ significant versus CTL.

published previously,[42] where experimental conditions of severe hypoxia induced an increased expression of VEGF.

Previously, we observed astroglial reaction to PA by both conventional transmission electron microscopy and light microscopy with immunohistochemistry for GFAP and tomato lectin histochemistry.[7] In agreement with those previous studies, GFAP was found in the internal processes of specialized astrocytes called Müller cells, which eventually form the internal limiting membrane.[7] In addition, it has been described that iNOS expression mediated by HIF-1 contributes to neuronal toxicity,[27] which could partly explain the neurodegeneration previously observed in ganglion cells.[7] With regard to GFAP, its expression was observed after 7 days of PA, localizing in the internal limiting membrane at PA-PND15, spreading to the perivascular glia of the IR and then to the inner processes of Müller cells at the IPL. GFAP increments were detected in the 7-day-old PA group in relation to CTL, whereas morphologic changes were detected later (15 days old), suggesting that molecular changes could precede morphologic alterations. The results of the present work suggest that in spite of other processes that may be associated with retinal thickening, the progressive thickening in the IR observed starting at postnatal day 15 may be due to a combination of angiogenesis and gliosis processes.

It has been extensively described that hypothermia is an effective method for short- and long-term sequelae prevention in the CNS of rats subjected to PA,[3,5,16] including retinal injury.[7,8] A possible mechanism of action to explain the neuroprotective effect of hypothermia is the inhibition of NO synthase activity and protein nitration.[3,8] The present work adds AM and VEGF expression inhibition by hypothermia as a key factor to preserve hypoxic retina from the damage generated by neovascularization. Experimental therapeutic strategies against ROP described in the literature include the use of antioxidants,[43] D-penicillamine,[44] allopurinol,[45] indomethacin,[46] dexamethasone,[47] rofecoxib,[48] and others. However, none of them proved to be as effective as hypothermia in preventing retinopathy. Recently, a trial employing therapeutic hypothermia was reported.[49] Neonates with hypoxic-ischemic encephalopathy who participated in the Total Body Hypothermia for Neonatal Encephalopathy (TOBY) trial were subjected to head cooling combined with whole-body cooling to 33.5°C for 72 hours.[50] Therapeutic hypothermia was shown to

decrease brain tissue injury, and to improve survival and neurological outcomes at up to 18 months of age.[49,51]

In conclusion, these results suggest that aberrant angiogenesis and exacerbated gliosis are factors implicated in the increased thickness of the IR as result of hypoxia-ischemia, whereas treatment with hypothermia is able to prevent those alterations. The highlight of the present research is that application of acute hypothermia prevents the development of retinal injuries, opening the possibility of a new therapeutic strategy if applied as soon as possible after the hypoxic injury. Future experiments will be carried out to explore the window of opportunity for hypothermia intervention to develop a useful protocol for clinical use.

Acknowledgments

We thank Andrea Pecile and Manuel Antonio Ponce for biomaterial assistance, Soledad Martínez Montero for her excellent technical assistance, and Roberto Fernández for his helpful assistance at confocal microscopy.

Supported by UBACyT 20020090100254 (CFL), PICTO 2009-0184 (CFL), Spain's Ministry of Science and Innovation Grant SAF2009-13240-C02-01 (AM), and Project SAF2010-15173 (RM-M).

Disclosure: **M. Rey-Funes**, None; **V.B. Dorfman**, None; **M.E. Ibarra**, None; **E. Peña**, None; **D.S. Contartese**, None; **J. Goldstein**, None; **J.M. Acosta**, None; **I.M. Larráyoz**, None; **R. Martínez-Murillo**, None; **A. Martínez**, None; **C.F. Loidl**, None

References

1. Cunningham, RG, Leveno, KJ, Ploom, SL, Gilstrap, LC, Hauth, JC, Wendstrom, KD. *Williams Obstetrics*. 22nd ed. New York: McGraw-Hill; 2005.
2. World Health Organization. *Consultation on Birth Asphyxia and Thermal Control of the Newborn*. Geneva, Switzerland: World Health Organization; 1990.
3. Dorfman VB, Rey-Funes M, Bayona JC, López EM, Coirini H, Loidl CF. Nitric oxide system alteration at spinal cord as a result of perinatal asphyxia is involved in behavioral disabilities: hypothermia as preventive treatment. *J Neurosci Res*. 2009;87:1260–1269.
4. Loidl CF, Herrera-Marschitz M, Andersson K, et al. Long-term effects of perinatal anoxia on basal ganglia neurotransmitter systems studied with microdialysis in the rat. *Neurosci Lett*. 1994;175:9–12.
5. Loidl CF, De Vente J, Markerink van Ittersum M, et al. Hypothermia during or after severe perinatal anoxia prevents increase in cyclic GMP-related nitric oxide levels in the newborn rat striatum. *Brain Res*. 1998;791:303–307.
6. Loidl CF, Danilo Gavilanes AW, Van Dijk EH, et al. Effects of hypothermia and gender on survival and behavior after perinatal anoxia in rats. *Physiol Behav*. 2000;68:263–269.
7. Rey-Funes, M, Ibarra, ME, Dorfman, VB, et al. Hypothermia prevents the development of ischemic proliferative retinopathy induced by severe perinatal asphyxia. *Exp Eye Res*. 2010; 90:113–120.
8. Rey-Funes M, Ibarra ME, Dorfman VB, et al. Hypothermia prevents nitric oxide system changes in retina induced by severe perinatal asphyxia. *J Neurosci Res*. 2011;89:729–743.
9. American Psychiatric Association. *Diagnostic and Statistical Manual of Mental Disorders, Third Edition (DSM-III)*. Washington, DC: American Psychiatric Association; 2001.
10. Younkin DP. Hypoxic-ischemic brain injury of the newborn—statement of the problem and overview. *Brain Pathol*. 1992;2: 209–210.
11. Hill A. Current concepts of hypoxic-ischemic cerebral injury in the term newborn. *Pediatr Neurol*. 1991;7:317–325.
12. Palmer C, Vannucci R. Potential new therapies for perinatal cerebral hypoxia-ischemia. *Clin Perinatol*. 1993;20:411–432.
13. Rivkin MJ. Hypoxic-ischemic brain injury in the term newborn. Neuropathology, clinical aspects, and neuroimaging. *Clin Perinatol*. 1997;24:607–625.
14. Ekimova IV. Changes in the metabolic activity of neurons in the anterior hypothalamic nuclei in rats during hyperthermia, fever, and hypothermia. *Neurosci Behav Physiol*. 2003;33: 455–460.
15. Gisselsson LL, Matus A, Wieloch T. Actin redistribution underlies the sparing effect of mild hypothermia on dendritic spine morphology after in vitro ischemia. *J Cereb Blood Flow Metab*. 2005;25:1346–1355.
16. Loidl CF. *Short and Long Term Effects of Perinatal Asphyxia*. Maastricht, The Netherlands: Maastricht University; 1997. Thesis.
17. Battin MR, Penrice J, Gunn TR, Gunn AJ. Treatment of term infants with head cooling and mild systemic hypothermia (35.0 degrees C and 34.5 degrees C) after perinatal asphyxia. *Pediatrics*. 2003;111:244–251.
18. Gunn AJ. Cerebral hypothermia for prevention of brain injury following perinatal asphyxia. *Curr Opin Pediatr*. 2000;12: 111–115.
19. Katz LM, Young AS, Frank JE, Wang Y, Park K. Regulated hypothermia reduces brain oxidative stress after hypoxic-ischemia. *Brain Res*. 2004;1017:85–91.
20. Kitamura K, Kangawa K, Kawamoto M, Ichiki Y, Nakamura S, Matsuo H. Adrenomedullin: a novel hypotensive peptide isolated from human pheochromocytoma. *Biochem Biophys Res Commun*. 1993;192:553–560.
21. López J, Martínez A. Cell and molecular biology of the multifunctional peptide, adrenomedullin. *Int Rev Cytol*. 2002;221:1–92.
22. Garayoa M, Martínez A, Lee S, et al. Hypoxia-inducible factor-1 (HIF-1) up-regulates adrenomedullin expression in human tumor cell lines during oxygen deprivation: a possible promotion mechanism of carcinogenesis. *Mol Endocrinol*. 2000;14:848–862.
23. Serrano J, Uttenthal LO, Martínez A, et al. Distribution of adrenomedullin-like immunoreactivity in the rat central nervous system by light and electron microscopy. *Brain Res*. 2000;853:245–268.
24. Udono-Fujimori R, Udono T, Totsune K, Tamai M, Shibahara S, Takahashi K. Elevated adrenomedullin in the vitreous of patients with diabetic retinopathy. *Requl Pept*. 2003;112:95–101.
25. Ito S, Fujisawa K, Sakamoto T, Ishibashi T. Elevated adrenomedullin in the vitreous of patients with diabetic retinopathy. *Ophthalmologica*. 2003;217:53–57.
26. Udono T, Takahashi K, Abe T, Shibahara S, Tamai M. Elevated immunoreactive-adrenomedullin levels in the aqueous humor of patients with uveitis and vitreoretinal disorders. *Peptides*. 2002;23:1865–1868.
27. Osborne N, Casson R, Wood J, Chidlow G, Graham M, Melena J. Retinal ischemia: mechanism of damage and potential therapeutic strategies. *Prog Retinal Eye Res*. 2004;23:91–147.
28. Hofman P, van Blijswijk BC, Gaillard PJ, Vrensen GF, Schlingemann RO. Endothelial cell hypertrophy induced by vascular endothelial growth factor in the retina: new insights into the pathogenesis of capillary nonperfusion. *Arch Ophthalmol*. 2001;119:861–866.
29. Semenza GL. Expression of hypoxia-inducible factor 1: mechanisms and consequences. *Biochem Pharmacol*. 2010; 59:47–53.
30. Loidl CF, Herrera-Marschitz M, Andersson K, et al. Short and long-term effects of perinatal asphyxia in rats monitored with peripheral and intracerebral microdialysis. *Amino Acids*. 1993;5:167.

31. Blom J, Giove TJ, Pong WW, Blute TA, Eldred WD. Evidence for a functional adrenomedullin signaling pathway in the mouse retina. *Mol Vis*. 2012;18:1339–1353.
32. Martínez A, Weaver C, López J, et al. Regulation of insulin secretion and blood glucose metabolism by adrenomedullin. *Endocrinology*. 1996;137:2626–2632.
33. Ishikawa T, Chen J, Wang J, et al. Adrenomedullin antagonist suppresses in vivo growth of human pancreatic cancer cells in SCID mice by suppressing angiogenesis. *Oncogene*. 2003;22: 1238–1242.
34. Martínez A, Julián M, Bregonzio C, Notari L, Moody TW, Cuttitta F. Identification of vasoactive non-peptidic positive and negative modulators of adrenomedullin using a neutralizing monoclonal antibody-based screening strategy. *Endocrinology*. 2004;145:3858–3865.
35. Roldós V, Martín-Santamaría S, Julián M, et al. Small molecule negative modulators of adrenomedullin: design, synthesis, and 3D-QSAR study. *Chem Med Chem*. 2008;3:1345–1355.
36. Pérez-Castells J, Martín-Santamaría S, Nieto L, et al. Structure of micelle-bound adrenomedullin: a first step toward the analysis of its interactions with receptors and small molecules. *Biopolymers*. 2012;97:45–53.
37. Höckel M, Vaupel PJ. Tumor hypoxia: definitions and current clinical, biologic, and molecular aspects. *J Natl Cancer Inst*. 2001;93:266–276.
38. Sapieha P, Hamel D, Shao Z, et al. Proliferative retinopathies: angiogenesis that blinds. *Int J Biochem Cell Biol*. 2010;42:5–12.
39. Chemtob S, Hardy P, Abran D, et al. Peroxide-cyclooxygenase interactions in postasphyxial changes in retinal and choroidal hemodynamics. *J Appl Physiol*. 1995;78:2039–2046.
40. Forsythe JA, Jiang BH, Iyer NV, et al. Activation of vascular endothelial growth factor gene transcription by hypoxia-inducible factor 1. *Mol Cell Biol*. 1996;16:4604–4613.
41. Vangeison G, Carr D, Federoff HJ, Rempe DA. The good, the bad, and the cell type-specific roles of hypoxia inducible factor-1 alpha in neurons and astrocytes. *J Neurosci*. 2008;28: 1988–1993.
42. Donahue ML, Phelps DL, Watkins RH, LoMonaco MB, Horowitz S. Retinal vascular endothelial growth factor (VEGF) mRNA expression is altered in relation to neovascularization in oxygen induced retinopathy. *Curr Eye Res*. 1996;15:175–184.
43. Raju TN, Langenberg P, Bhutani V, Quinn G. Vitamin E prophylaxis to reduce ROP: a reappraisal of published trials. *J Pediatrics*. 1997;131:844–850.
44. Phelps DL, Lakatos L, Watts JL. D-Penicillamine for preventing retinopathy in preterm infants. *Cochrane Database Syst Rev*. 2000;2:CD001073.
45. Russell GA, Cooke RW. Randomised controlled trial of allopurinol prophylaxis in very preterm infants. *Arch Dis Child Fetal Neonatal Ed*. 1995;73:F27–F31.
46. Nandgaunkar BN, Rotschild T, Yu K, Higgins RDI. Indomethacin improves oxygen-induced retinopathy in the mouse. *Pediatr Res*. 1999;46:184–188.
47. Rotschild T, Nandgaunkar BN, Yu K, Higgins RD. Dexamethasone reduces oxygen induced retinopathy in a mouse model. *Pediatr Res*. 1999;46:94–100.
48. Wilkinson-Berka JL, Alousis NS, Kelly DJ, Gilbert RE. COX-2 inhibition and retinal angiogenesis in a mouse model of retinopathy of prematurity. *Invest Ophthalmol Vis Sci*. 2003; 44:974–979.
49. Edwards AD, Brocklehurst P, Gunn AJ, et al. Neurological outcomes at 18 months of age after moderate hypothermia for perinatal hypoxic ischaemic encephalopathy: synthesis and meta-analysis of trial data. *BMJ*. 2010;340:c363.
50. Azzopardi D, Brocklehurst P, Edwards D, et al; TOBY Study Group. The TOBY Study. Whole body hypothermia for the treatment of perinatal asphyxial encephalopathy: a randomised controlled trial. *BMC Pediatr*. 2008;8:17.
51. Rutherford M, Ramenghi LA, Edwards AD, et al. Assessment of brain tissue injury after moderate hypothermia in neonates with hypoxic-ischaemic encephalopathy: a nested substudy of a randomised controlled trial. *Lancet Neurol*. 2010;9:39–45.

Investigative Ophthalmology & Visual Science